Studies on Models for Tetrahydrofolic Acid. 7. Reactions and Mechanisms of Tetrahydroquinoxaline Derivatives at the Formaldehyde Level of Oxidation

T. H. Barrows, P. R. Farina, R. L. Chrzanowski, P. A. Benkovic, and S. J. Benkovic*

Contribution from the Department of Chemistry, The Pennsylvania State University, University Park, Pennsylvania 16802. *Received July 1, 1975*

Abstract: Trapping of the formaldehyde condensation product, ethyl *p*-(3,4,4a,5-tetrahydroimidazo[1,5-*a*]quinoxalin-2(1*H*)-yl)benzoate (**2a**) in aqueous solution (pH 1–8) by sodium cyanoborohydride yields a single *N*-methyl product (at N-1 of the tetrahydroquinoxaline ring) which was identified by comparison with the two possible *N*-methyl isomers. The N-1 methyl compound reacts with formaldehyde at the N-4 and N-10 positions to give a benzotriazocine adduct (hexahydropyrimidine) whose chair conformation and stability were elucidated by high resolution NMR and kinetic studies, respectively. Below pH 2, **2a** undergoes an irreversible rearrangement through the N-1 iminium cation to yield 2-carbethoxy-5,6,7,8-tetrahydro-14*H*-quinoxo[2,1-*c*][1,4]benzodiazepine. Crossover experiments indicate that the methylene bridge of **2a** is completely exchanged with added formaldehyde before yielding the benzodiazepine. The above results were interlocked with further investigations of the kinetics for condensation of formaldehyde with various para-substituted tetrahydroquinoxaline derivatives under conditions both first and zero order in formaldehyde concentration. It was demonstrated that benzotriazocine formation competes with synthesis of the imidazolidine adducts across the series. Structure–reactivity correlations were obtained that demonstrate: (1) the interconversion of benzotriazocine and imidazolidine is through formaldehyde and not an intramolecular rearrangement; (2) the exocyclic nitrogen (N-10) catalyzes the condensation of formaldehyde at the N-1 tetrahydroquinoxaline nitrogen; and (3) ring opening of the imidazolidine adduct is directed to the more stable iminium cation under kinetic and thermodynamic control. The overall mechanism then involves a reaction cascade ultimately under thermodynamic control: parent amine → benzotriazocine → imidazolidine → benzodiazepine. The initial kinetic control is imposed by differences in the condensation-cyclization rates at the tetrahydroquinoxaline nucleus but the overall sequence proceeds through intermolecular reactions mediated by free formaldehyde. The implications of these results to the mechanism of action of the natural cofactor are discussed.

In previous investigations we have discussed the condensation of formaldehyde with various 2-[*p*-(anilino)methyl]-1,2,3,4-tetrahydroquinoxaline derivatives as possible model systems for the tetrahydrofolic acid–5,10-methylenetetrahydrofolic acid interconversion.[1,2] The work reported here bears on: (1) the identity of the nitrogen site for the iminium cation formed under kinetic or thermodynamic control in the ring cleavage of dissymmetric imidazolidine adducts; (2) the further acid catalyzed rearrangement of the imidazolidine adduct; (3) the synthesis, characterization, and properties of a benzotriazocine (hexahydropyrimidine) and its relationship to the mechanism of formaldehyde condensation with the tetrahydroquinoxaline derivatives; and (4) the assessment of electronic effects on the condensation with formaldehyde through the extension of the previous investigations to obtain reaction parameters both dependent and independent of formaldehyde concentration.[1] By studying both the formation and ring opening reactions of various imidazolidine and benzotriazocine adducts, a detailed description of the mechanism is now possible.

Results

a. Structures. The parent tetrahydroquinoxalines (**1a–c**) employed were those obtained earlier;[1,2] the synthesis of **1d** followed identical procedures. The imidazolidines (**2a–c**) likewise were those described previously; the synthesis of **2d** was accomplished similarly. The assignment of the five-membered ring structure is based mainly on the NMR spectra of these compounds, namely the appearance of the $-NCH_2N-$ resonance centered at δ 4.72 (J_{ab} = 4 Hz), 4.63 (J_{ab} = 4 Hz), and 4.72 (J_{ab} = 4 Hz) for **2a, 2c,** and **2d,** respectively. The geminal coupling constant (J_{ab} = 4–5 Hz) is diagnostic of ring size.[1] The syntheses of the tetrahydroquinoline derivative (**3**) and imidazolidine (**4**) related to **1a** also have been reported earlier.[2] A key feature of the NMR spectrum of the latter, **4**, is the $-NCH_2N-$ absorption as an AB quartet, δ 4.52 (J_{ab} = 4 Hz), validating the use of the coupling constant in this structural series.

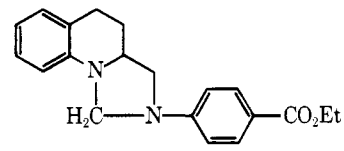

4

The examination of the direction of ring opening of **2a** employed cyanoborohydride as a trapping reagent, thereby necessitating the synthesis of the two isomeric methyl derivatives. The N-1 and N-10 formyl derivatives of **1a** have been synthesized and characterized previously.[3] Reduction of either formyl isomer in tetrahydrofuran with diborane generated in situ appears to be rapid and quantitative at room temperature.[4] Equilibration of the isomers via the formamidinium salt is prevented by completing the diborane generation via the reaction of boron trifluoride with excess sodium borohydride[5] in tetrahydrofuran prior to the addition of the formyl isomer. Formation of the N-1 (**5**) or N-10 (**6**) methyl product is evident from (a) the disappearance of the formyl proton absorption at δ 8.9 (N-1) or 8.6 (N-10) and the appearance of a methyl singlet at δ 2.9 (N-1) or 3.0 (N-10) in $CDCl_3$ and (b) changes in the ultraviolet spectra from λ_{max} (H_2O) 307 nm (ϵ 25 700) and 300 nm (ϵ 4400) at pH 7.0 for the N-1 and N-10 formyl isomers, respectively, to λ_{max} (50% v/v dioxane–water) 312

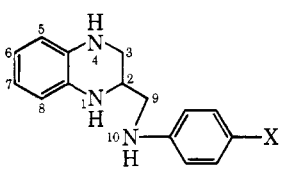

1a, X = CO_2Et
b, X = Cl
c, X = CH_3
d, X = CN

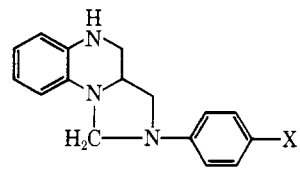

2a, X = CO_2Et
b, X = Cl
c, X = CH_3
d, X = CN

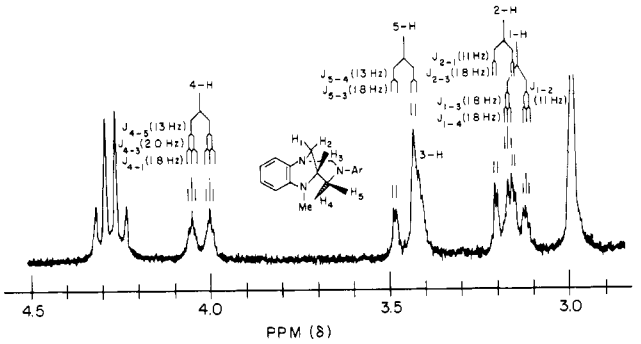

Figure 1. Spectrum of 7-d_2 in the region of 4.1 to 3.1 ppm.

nm (ε 24 800) at pH 7.0 and λ_{max} (EtOH) 314 nm (ε 31 400) for the corresponding *N*-methyl isomers. The uv spectra of **1a** and **2a** exhibit λ_{max} (EtOH) at 308 nm (ε 25 400) and λ_{max} (50% v/v dioxane–water) 310 nm (ε 32 900) at pH 7.0, respectively; thus the bathochromic shifts are consistent with the anticipated chemical modification.[1,2] Although changes in the NMR spectra of the two compounds are suggestive of the site of *N*-methylation, the loss of the near singlet corresponding to the four aromatic protons of the tetrahydroquinoxaline moiety in **1a** upon substitution at N-1 but not at N-10 is not uniquely definitive as in the case of the formyl or formimidoyl isomers.[3,6] However, comparison of the observed chemical shift differences ($\delta B - \delta A$) in the AB pattern arising from the *p*-aminobenzoate moiety for the two isomers reveals a greater separation for the N-1 methyl isomer in agreement with earlier results.[6] Further structural proof was sought by chemical derivatization.

Treatment of **5**, the N-1 methyl isomer, with formaldehyde yields a crystalline adduct after chromatographic purification, whereas **6**, the assigned N-10 methyl isomer, does not. Since a methylene bridge between N-1 and N-4 does not readily form in the tetrahydroquinoxaline system (in fact a dimer and not the 1,4-methylene derivative has been obtained[7]), the formation of **7** further supports the assignment of the sites of N-methylation. The benzotriazocine structure assigned to **7** was deduced from the following information.

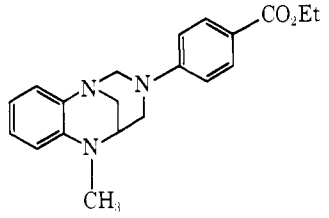

7

Absorptions due to NH stretch are absent in the ir spectrum of **7**. The NMR spectrum of the four aromatic protons of the tetrahydroquinoxaline moiety reveals a wide multiplet for **7**, whereas the N-1 methyl derivative (**5**) exhibits much less splitting and the parent unsubstituted compound (**1a**) gives a near singlet. The appearance of a new ultraviolet maximum (50% v/v dioxane–water) at pH 7.0 at 258 nm as well as the decrease in absorption at 312 nm (ε 21 800) with respect to **5** is expected due to restriction of the resonance of N-4 with the phenyl ring.[1] Monoprotonation of **1a** provides an example for loss of conjugation and results in a hypsochromic shift of λ_{max} (H_2O) from 308 to 302 nm and a 6% decrease in the intensity of the band.[1]

Condensation of formaldehyde-d_2 with **5** yields a material identical with **7** except for the mass spectral parent peak which is two units higher. The AB quartet at 4.84 and 4.32 (J = 12 Hz) for **7** is absent in the NMR spectrum of 7-d_2 while the remaining portions of the two spectra are superimposable. This

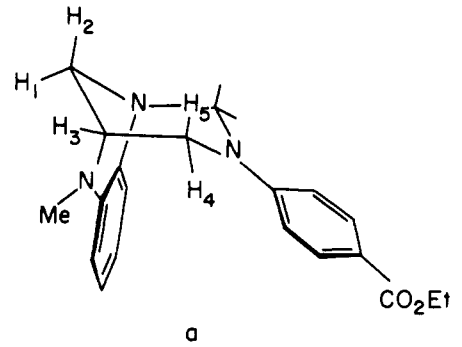

a

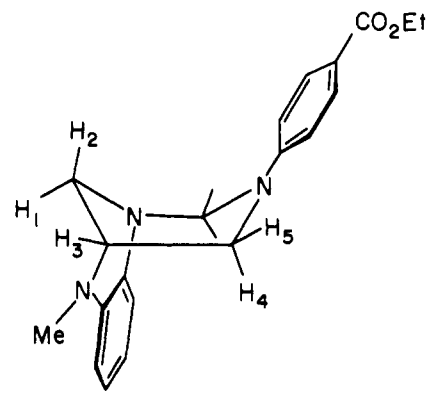

b

Figure 2. Two possible limiting conformations, a and b, for **7**.

observation identifies the protons of the 4,10-methylene bridge. The geminal coupling constant of J_{ab} = 12 Hz for **7** is consistent with a hexahydropyrimidine structure (for *N,N'*-dimethylhexahydropyrimidine, J_{ab} = 9 Hz,[8] and for trimethylhexahydro-1,3,5-triazine,[9] J_{ab} = 10 Hz) and contrasts with those listed above for the five-membered imidazolidines.

The remaining five aliphatic protons can be tentatively identified upon examination of a 250-MHz NMR spectrum of 7-d_2 in the region of 4.1 to 3.1 ppm (Figure 1). The AB quartet at δ 4.01 (1 H) and 3.47 (2 H) (J = 13 Hz) is assigned as the 4-H and 5-H protons with 3-H overlapping at δ 3.42. The multiplet centered at δ 3.17 (2 H) is attributed to the 1-H and 2-H protons. The 4-H and 5-H protons appear downfield relative to 1-H and 2-H since the former are adjacent to the more electronegative nitrogen.[10] In addition, a Dreiding molecular model of **7** in either of two possible limiting conformations (Figure 2) shows that the 1-H and 2-H protons are above the plane of the tetrahydroquinoxaline aromatic ring. This places 1-H and 2-H within a shielding region[10] and rationalizes their higher field chemical shifts. The model also shows that in the chair conformation of **7**, 3-H bisects the angle formed between 1-H and 2-H as well as the angle formed between 4-H and 5-H to give dihedral angles of ca. 55° in each case. The Karplus relationship predicts that vicinal coupling constants for this angle should be about J = 2.3 Hz.[10] Vicinal coupling constants of 1.8 Hz[11] are observed for all four protons coupled to 3-H which is consistent with the model and suggests that conformation a rather than b is being observed.

If **7** preferentially adopts conformation a, then given the rigidity of the structure, the possibility arises for long-range coupling to occur between 1-H and 4-H. Observed W coupling of the 4-H and 1-H protons (1.8 Hz) falls within the 0–3 Hz values associated with this phenomenon,[10] permitting a definitive assignment of the resonances attributed to 4-H and 1-H. The U-shaped orientation of 2-H and 5-H prevents cou-

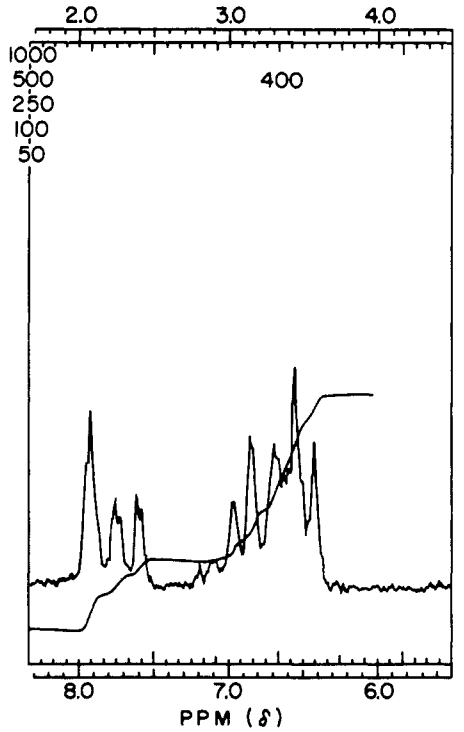

Figure 3. The NMR absorption pattern in the aromatic region for **9** at 60 MHz.

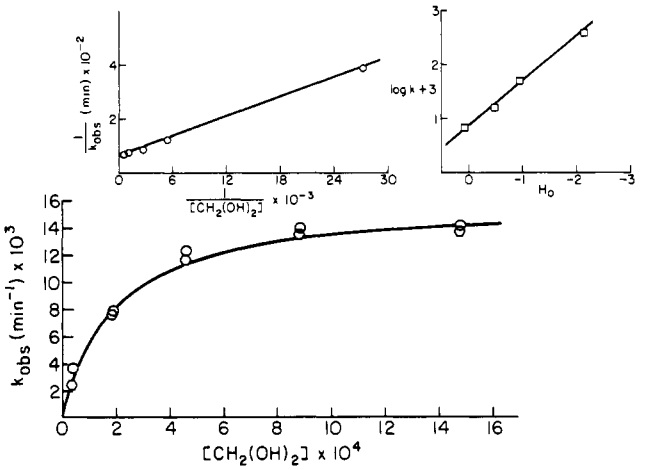

Figure 4. Lower curve: plot of k_{obsd} vs. $[CH_2(OH)_2]$ at H_0 −0.47, 25 °C, for formation of **8** where O represents reactions initiated with **2a** and O reactions initiated with **1a**. Upper left insert: Plot of k_{obsd}^{-1} vs. $[CH_2(OH)_2]^{-1}$ at H_0 −0.47, 25 °C, where the ordinate intercept equals $(k_7k_{1M}/k_{-1M})^{-1}$ and the intercept at the abscissa, $-(k_{1M}k_5/k_{-1M}k_{-5})$. Upper right insert: Graph of k_{obsd} at saturating $[CH_2(OH)_2]$ as a function of H_0, 25 °C. Solid lines calculated from values listed in the Results and eq 1.

pling between the protons. The identification of 4-H as the downfield proton is also supported by examination of conformation a. Conjugation between the N-10 lone pair electrons and the benzocaine aromatic ring is expected to fix the plane of the ring in a position perpendicular to the nitrogen lone pair. Evidence for conjugation is provided by the ir absorption of 1690 cm^{-1} for **7** which indicates considerable single bond character for the C=O group. The C=O absorption band typically is 1750–1735 cm^{-1} for saturated aliphatic esters and 1730–1715 cm^{-1} for aryl esters.[12] This requirement places 4-H rather than 5-H in a deshielded region when **7** is in the chair conformation a, but the positions are reversed if **7** is in the boat conformation b. Furthermore, the boat conformation would (1) not account for the observed long-range coupling if the resonance at δ 4.01 is now assigned to 5-H and (2) would nearly eclipse the 3-H and 5-H protons that would result in a large difference (ca. 5 Hz) between the vicinal coupling constants J_{5-3} and J_{4-3}.[10]

Treatment of **2a** or **4** with aqueous acid leads to the rearranged benzodiazepine products **8** and **9**, respectively. The proof of structure will be illustrated for **9** although analogous evidence obtains for **8**. The benzodiazepine **9** exhibits an AXX′

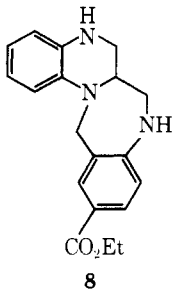

8

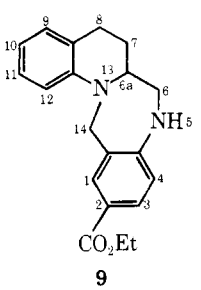

9

NMR absorption pattern in the aromatic proton region characteristic of an unsymmetrical trisubstituted benzene ring (Figure 3). The 1-H and 3-H protons appear at δ 7.95 and 7.60 downfield from the complex multiplet that contains the remaining five aromatic protons. The two 14-H protons are found as a singlet at δ 4.58 which is absent in the NMR spectrum of the corresponding **9**-d_2 analogue prepared from **4**-d_2 which is dideuterated at the bridging carbon (C-1). The ir spectrum of **9** exhibits N–H stretching at 3400 cm^{-1} which is absent in the ir spectrum of **4**. The uv spectra of **9** and **4** reveal the anticipated changes in the long wavelength absorption associated with ortho substitution of the benzocaine moiety that tend to inhibit resonance of N-1 with the aromatic ring. This band shifts from λ_{max} (EtOH) 304 nm in **4** to 302 nm in **9** with a corresponding decrease in intensity (ϵ 38 000 to ϵ 22 000).

b. Kinetics. 1. Trapping with NaCN(BH$_3$). Reductive trapping of the iminium cation(s) formed initially by ring cleavage of the imidazolidine (**2a**) prior to its hydration to the carbinolamine was carried out with sodium cyanoborohydride, owing to its greater stability relative to borohydride in acidic aqueous media and its ability to rapidly reduce the iminium cation species.[13] Addition of stock solutions of **2a** to 50% v/v dioxane–water buffers containing excess sodium cyanoborohydride at pH 1.6, 4.2, and 7.3 gave the N-1 methyl product and no detectable (<5%) N-10 isomer. The first-order rate constants, obtained as a function of cyanoborohydride concentration by monitoring the change in the uv spectrum at 310 nm, remain first order in cyanoborohydride concentration as the latter is varied within practical limits ($\gtrsim 10^{-3}$ M). Consequently the species trapped may not correspond to that initially formed (see Discussion).

2. Benzodiazepine Formation. The observed rate constants for formation of **8** (monitored at 300 nm) from either **2a** or **1a** exhibit a change from a first-order to a zero-order dependency on formaldehyde concentration at a constant pH (Figure 4). At saturating formaldehyde levels, k_{obsd} is a linear function of H_0 with a slope of unity. These observations are accommodated by Scheme I, which includes an iminium species based on mechanistic grounds rather than required by the observed kinetic behavior.

Assuming the N-1 iminium cation to be at a steady state level and $k_7 \ll k_5$ or k_{-1M}[14] then

$$k_{obsd} = k_7k_{1M}k_{-5}\left[\frac{H_0[CH_2(OH)_2]}{k_{1M}k_5[CH_2(OH_2] + k_{-1M}k_{-5}}\right] \quad (1)$$

Table I. Crossover Experiments for the Formation of Benzodiazepines **8** and **9** from Imidazo[1,5-*a*] Adducts **2a** and **4**

Run	H_0	Reactant (mmol)	$CD_2(OH)_2$, mmol	$CH_2(OH)_2$, mmol	324/322 or 325/323
1	0.48	**4**-d_2 (0.1)		0.3	0.46[a]
2	0.48	**4**-d_2 (0.1)		0.1	0.68[a]
3	0.48	**4** (0.1)	0.3		1.25[a]
4	0.48	**4** (0.1)	0.1		0.73[a]
5	1.47	**4** (0.1)	0.3		1.88[a]
6	0.48	**3** (0.1)	0.3	0.1	1.63[a]
7	−0.47	**2a** (0.1)	0.3		2.65[b]
8	−0.47	**2a** (0.1)	0.5		4.40[b]
9	0.48	**2a** (0.1)	0.3		2.84[b]

[a] 324/322. [b] 325/323.

Scheme I

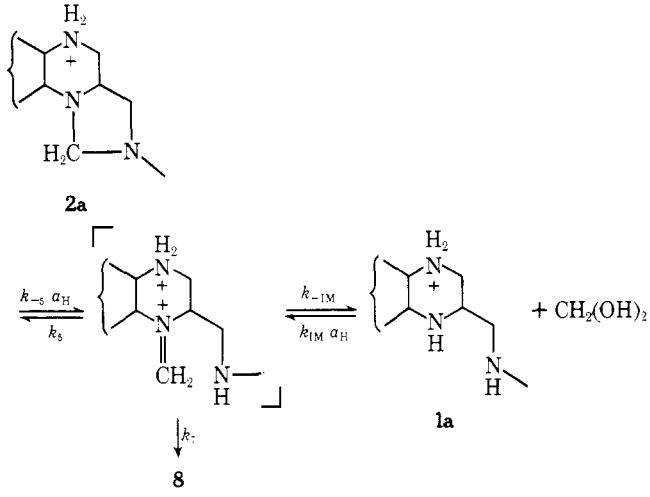

where $[CH_2(OH)_2]$ represents the concentration of formaldehyde as the hydrate,[15] and H_0 the activity of hydrogen ion as measured by the H_0 acidity function. Values of $k_7k_{IM}k_{-5}$ and $k_{IM}k_5/k_{-IM}k_{-5}$ employed to calculate the solid lines in Figure 4 were 1.60×10^{-2} M^{-3} min^{-3} and 5.10×10^3 M^{-1}, respectively. Although the latter term decreases with increasing H_0 ($H_0 = -2.15$, $k_{IM}k_5/k_{-IM}k_{-5} = 1.0 \times 10^3$), the change is only a factor of 5 whereas a_H has increased by greater than 10^2. Since the pK_a values of **1a** assigned to the N-1/N-4 and N-10 nitrogens are 4.35 and −0.33[1] and change by ca. −1 pK_a unit upon forming **2a**,[1] it is conceivable that the monoprotonated species of **2a** and **1a** rather than the free base forms are the reactive pair in the acidity region. The limited variation in H_0 imposed by accessible rate measurements precludes a choice between these alternatives; consequently the $k_{IM}k_5/k_{-IM}k_{-5}$ term is not a reliable measure of the **1a–2a** equilibrium.

The assumption of the establishment of a preequilibrium prior to benzodiazepine formation was tested in a series of crossover experiments employing $[CD_2(OH)_2]$ or **4**-d_2 (at C-1) as the labeled materials. Pertinent results are listed in Table I with the corrected parent peak ratio (see Experimental Section) determined by mass spectrometric analysis serving as an index of deuterium incorporation. Comparison of runs 2 with 4 and 3 with 5 and 6 for the quinoline derived benzodiazepine indicates approximately the same incorporation of deuterium in **9** whether the initial reagent is the parent amine **3** or the imidazolidine adduct **4** or **4**-d_2 in accord with the preequilibrium postulate. The data from run 5 demonstrate the absence of a significant acidity effect on deuterium incorporation. Runs 7–9 for the quinoxaline derivative likewise reveal extensive incorporation of deuterium. The data may be treated graphically, i.e., as log plots of the molecular weight ratios vs. $[CD_2(OH)_2]/[CH_2(OH)_2]$. The latter are linear with slopes of unity and indicate a secondary deuterium isotope effect of 0.8 ± 0.1 in the two cases, accounting for the deviation from a statistical distribution. The effect is in the correct direction for a change from sp^2 to sp^3 hybridization at the α carbon, although the step(s) contributing to the effect is not readily separated.[16]

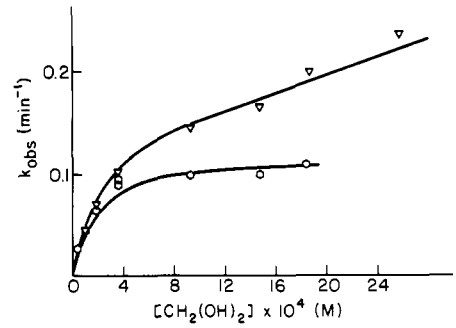

Figure 5. Plot of k_{obsd} vs. $[CH_2(OH)_2]$ for the formation of **2d**. Upper line (△) data at 0.08 M formate, pH 5.10; lower line (○) at 0.08 M acetate, pH 6.06 (50% v/v dioxane-H_2O, μ = 0.2, 25 °C). Solid line calculated from eq 2.

3. Condensation of Formaldehyde with 1d,c,a. The pseudo-first-order rate constant (k_{obsd}) for formation of the formaldehyde adduct from **1d** (*p*-CN) was determined spectrophotometrically from the time dependent increase in absorbance at 290 nm (50% v/v dioxane-H_2O, μ = 0.2, 25 °C), conditions identical with previous studies.[1] In the case of **1d**, as also noted for **1a–c**, k_{obsd} changes from first order to zero order in formaldehyde concentration as the latter is varied from 0 to 1.74×10^{-3} M over the pH range 6.0–9.1. At pH <6.0, saturation with formaldehyde is not achieved; instead a second process, first-order in $[CH_2(OH)_2]$, is apparently superimposed on the initial condensation reaction. An example of both types of behavior is depicted in Figure 5. The data are described in terms of Scheme II with the structure [**1d**·CH_2] specified below.

Scheme II

$$\mathbf{1d} + CH_2(OH)_2 \overset{K^6_{eq}}{\rightleftharpoons} [\mathbf{1d} \cdot CH_2] \xrightarrow{k', k^F[CH_2(OH)_2]} \mathbf{2d}$$

From Scheme II eq 2 for k_{obsd} may be derived where k' and k^F represent the rate coefficients associated with the nonformaldehyde and formaldehyde catalyzed conversion of [**1d**·CH_2] to **2d**, respectively.

$$k_{obsd} = [CH_2(OH)_2]\left[\frac{k'K^6_{eq} + k^FK^6_{eq}[CH_2(OH)_2]}{1 + K^6_{eq}[CH_2(OH)_2]}\right] \quad (2)$$

Both k' and k^F are pH and buffer dependent.[17] Linear extrapolation of k_{obsd} at saturating $[CH_2(OH)_2]$ to zero buffer

Table II. Calculated Values for the Rate Constants Employed in Equations 2-4 for the Formaldehyde Condensation with **1d**

Parameter	Numerical[a]	Parameter	Numerical[a]
K^6_{eq}, M^{-1}	5.4×10^3	B, min^{-1}	2.10×10^{-2}
k', min^{-1}	1.39×10^{-1},[b] 1.20×10^{-1} [c]	C, M	3.72×10^{-8}
k^F, M^{-1} min^{-1}	37.4[b]	k_{HB}, M^{-1} min^{-1}	2.0[d]

[a] Experiments in 50% v/v dioxane-H_2O, μ = 0.2, 25 °C. [b] At 0.08 M formate, pH 5.10. [c] At 0.08 M acetate, pH 6.06. [d] For acetic acid, pK_a = 6.06.

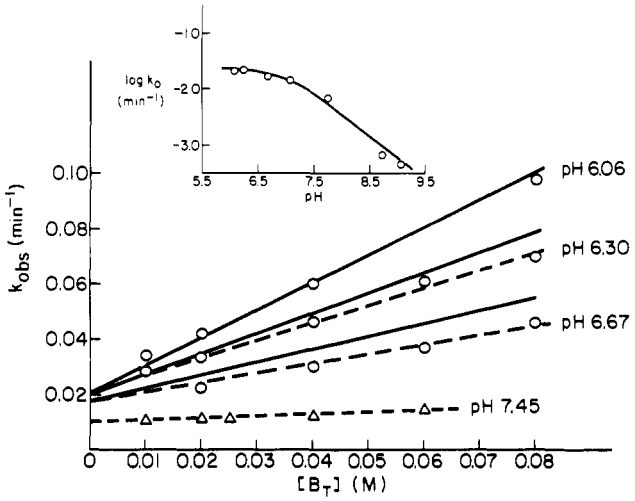

Figure 6. Plot of k_{obsd} for the condensation of $CH_2(OH)_2$ (saturating) with **1d** as a function of total buffer concentration for (○) acetate and (△) phosphate. Solid line calculated from eq 4; - - - extrapolation to obtain k_0. Upper insert: Graph of log k_0 against pH with the solid line computed from eq 3.

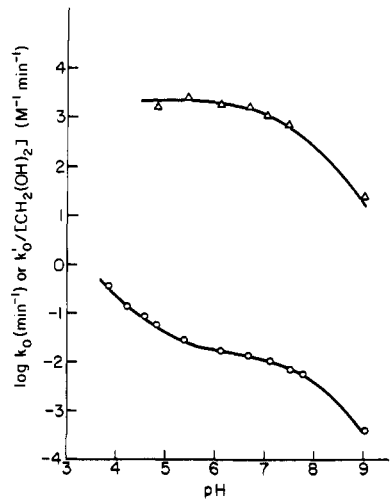

Figure 7. Upper curve: Graph of $k'_0/[CH_2(OH)_2]$, the second-order rate constant for formation of the benzotriazocine from **1a**, vs. pH. Lower curve: Plot of k_0 at saturating $[CH_2(OH)_2]$ for synthesis of imidazolidine, **2a** (50% v/v dioxane-H_2O, μ = 0.2, 25 °C).

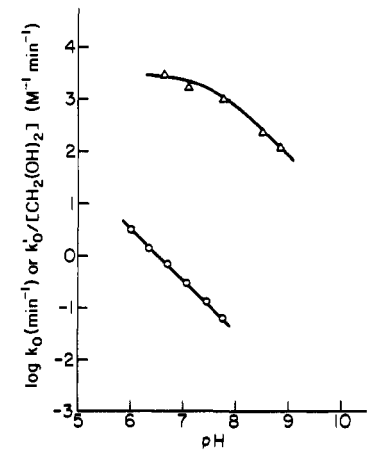

Figure 8. Upper curve: Graph of $k'_0/[CH_2(OH)_2]$, the second-order rate constant for formation of the benzotriazocine from **1c**, vs. pH. Lower curve: Plot of k_0 at saturating $[CH_2(OH)_2]$ for synthesis of imidazolidine, **2c** (50% v/v dioxane-H_2O, μ = 0.2, 25 °C).

concentration at pH values where k^F is negligible yields the pH dependent component of k' defined as k_0. The linear dependence of k_{obsd} on acetate and phosphate buffer concentrations as well as the derived pH-k_0 profile (insert) are illustrated in Figure 6. The pH behavior of k_0 can be satisfactorily simulated by the following general expression[1] where A = 0 in the present case owing to the experimental limitation.

$$k_0 = [Aa_H + B]a_H/(a_H + C) \quad (3)$$

The dependence of k_{obsd} on buffer concentration is simply rationalized by

$$k_{obsd} = k_{HB}[HB] + k_0 \quad (4)$$

with the buffer acting as a general acid catalyst. Values for the above rate coefficients and parameters are included in Table II. The break in the pH rate profile for k_0 occurs in a pH region well removed from the pK'_a for **1d.** Spectrophotometric titration of **1d** at 240 and 283 nm established macroscopic pK'_a values of 4.22 and −0.84 in water (25 °C) that were assigned on the basis of earlier arguments[1] to the monoprotonation of the N-1/N-4 quinoxaline nitrogens and the exocyclic nitrogen, respectively.

As noted previously,[1,2] the formation of **2** proceeds through a lag phase at early times which appears in plots of OD against time used to calculate k_{obsd}. This phase associated with synthesis of the initial condensation product is particularly accessible for **1a** and **1c** at the wavelengths (310, 290 and 255 nm) employed to monitor the production of the respective imidazolidines permitting the calculation of the pseudo-first-order constant, k'_{obsd}, for the synthesis of [**1a,c**·CH_2]. In Figures 7 and 8, the behavior of k'_{obsd} extrapolated to zero buffer concentration for the initial phase and expressed as $k'_0/[CH_2(OH)_2]$ is presented as a function of pH for **1a** (*p*-COOEt) and **1c** (*p*-CH_3). Over the formaldehyde concentrations employed (0-1.47 × 10^{-3} M) the initial condensation reaction remains first order in formaldehyde. The data for both derivatives are rationalized in terms of Scheme III,

Scheme III

$$CH_2(OH)_2 + \mathbf{1a,c} \underset{k'_{-4}}{\overset{k'_4}{\rightleftharpoons}} [\mathbf{1a,c} \cdot CH_2OH] \xrightarrow{k^c{}_4 a_H} [\mathbf{1a,c} \cdot CH_2]$$

which yields eq 5 for k'_0. Values for the rate constants are reported in Table III.

$$k'_0/[CH_2(OH)_2] = \frac{k'_4 k^c{}_4 a_H}{k'_{-4} + k^c{}_4 a_H} \quad (5)$$

Table III. Values of the Rate Coefficients for the Tetrahydroquinoxaline Series, **1a–d**, According to Scheme IV

	p-CN	*p*-COOEt	*p*-Cl	*p*-CH_3
k_1, M^{-2} min^{-1}		1.3×10^7	6.0×10^8	$(8.2 \times 10^9)^a$
k'_1, M^{-1} min^{-1}	1.1×10^2	6.9×10^1	5.4×10^1	
$k_1 k^c_1 / k_{-1}$, M^{-2} min^{-1}	3.1×10^9	2.3×10^9	4.5×10^9	$(8.2 \times 10^9)^a$
k'_4, M^{-1} min^{-1}		2.0×10^3		3.0×10^3
$k'_4 k^c_4 / k'_{-4}$, M^{-2} min^{-1}		2.8×10^{10}		8.7×10^{10}
K^6_{eq}, M^{-1}	5.4×10^3	5.5×10^3	6.0×10^3	2.6×10^3

[a] See Discussion.

Scheme IV

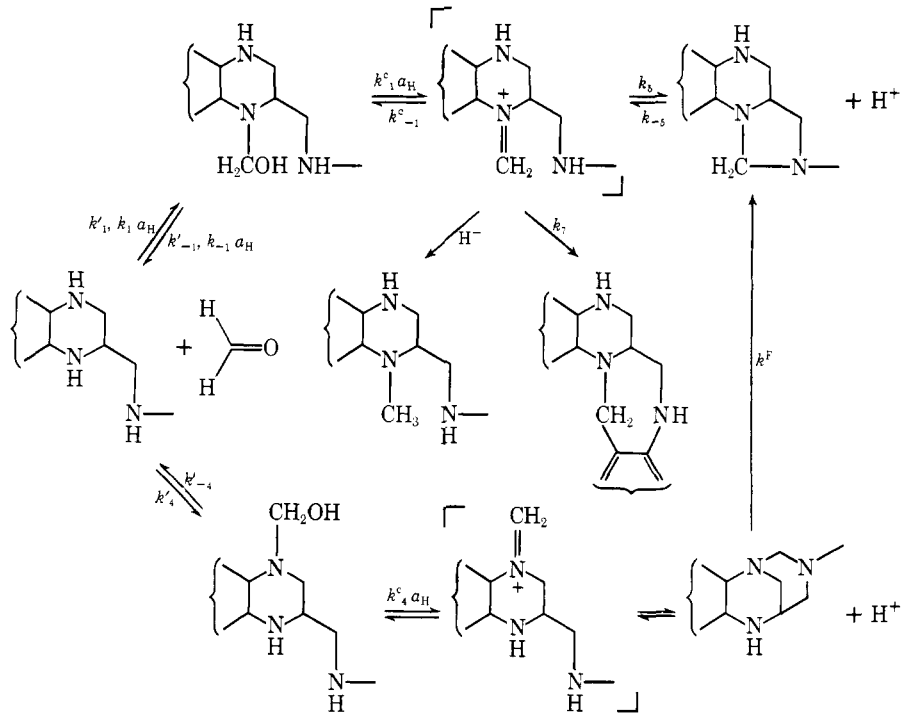

4. Equilibrium Constant for Formation of 7. The equilibrium constant for formation of the benzotriazocine, **7**, was calculated from the rate constants obtained for the formation and hydrolysis of **7**. The hydrolysis reaction was monitored spectrophotometrically by the time-dependent increase in absorbance at 312 nm. Runs were carried out in buffer solutions (50% v/v dioxane–water, pH 7.0, μ = 0.2, 25 °C) containing 0.02, 0.05, and 0.10 M mercaptoethanol with a substrate concentration of 5×10^{-5} M. The rate constant for hydrolysis obtained by extrapolation to zero buffer concentration equals 7.60×10^{-3} min^{-1} and was independent of mercaptoethanol concentration. The pseudo-first-order rate constants for formation of **7** and **5** and formaldehyde were determined from the time-dependent decrease in absorbance at 312 nm under identical conditions. Formaldehyde concentration was varied from 1.3×10^{-3} to 0.30 M and the rate constants were extrapolated to zero buffer concentration. The second-order rate constant (1.29×10^2 M^{-1} min^{-1}) for formation of the adduct was taken as the slope of a plot of the extrapolated rate constants vs. formaldehyde concentration where the reaction is first order in formaldehyde. The equilibrium constant (K^6_{eq}) for the formation of **7** defined in terms of stoichiometric concentration of formaldehyde therefore is 1.70×10^4 M^{-1}. The extrapolated rate constants for formation of **7** change from first order to zero order in formaldehyde concentration as the latter is varied from 0 to ca. 0.06 to 0.30 M at pH 7.0. A reciprocal plot gave K^c_4 = 23 ± 8 M^{-1} as the negative of the intercept at the abscissa. This value is interpreted as the equilibrium constant for carbinolamine formation at N-4 and falls within the range of 2–40 M^{-1} determined for cyclic secondary amines.[18]

Discussion

The overall mechanism for the various transformations of the tetrahydroquinoxaline derivatives in the presence of formaldehyde or as the adducts is presented in Scheme IV. Discussion of the evidence in support of Scheme IV described in this and earlier studies is conveniently divided into three areas based on the principal compounds formed, i.e., benzodiazepine, benzotriazocine, and imidazolidine. The discussion focuses on the chemistry of **1a**, the most appropriate model for tetrahydrofolate, although the arguments apply to all members in the series.

a. Benzodiazepine Formation. At low pH (<2), **2a** as well as the quinoline adduct **4** undergoes acid-catalyzed rearrangement in greater than 70% yield to the corresponding benzodiazepine derivatives. The rate for formation of **8** is identical whether the reaction is initiated with either the imidazolidine adduct (**2a**) or the parent amine (**1a**) plus formaldehyde consistent with establishment of a preequilibrium between the diamine and imidazolidine species, i.e., $k_7 < k^c_{-1} k_{-1} a_H$ or k_5. Additional evidence in support of this hypothesis is furnished by (a) the results of crossover experiments with $[CD_2(OH)_2]$ or the imidazolidine adducts dideuterated at C-1 that reveal, after correction for a secondary isotope effect, statistical distribution of the label in the isolated benzodiazepine owing to an equilibrated formaldehyde pool and

(b) initial rapid changes in the uv spectrum commencing with either **2a** or **1a** plus formaldehyde to give a superimposable spectrum before measurable formation of **8**.[14,19] The rate constants in Scheme I are simply equated with those in Scheme IV through the relationship $k_{IM}/k_{-IM} = k_1k^c{}_1/k_{-1}k^c{}_{-1}$.

A plausible mechanism for benzodiazepine formation in analogy with numerous examples of electrophilic aromatic substitution[20] envisions electrophilic attack by the N-1 iminium cation on the ortho position of the exocyclic aromatic ring leading to cyclization. Although the structure of the product implicates the N-1 cation, this finding does not rule out that the initial ring opening of **2a** might yield the N-10 iminium cation, since cyclization of the latter at C-8 of the tetrahydroquinoxaline ring would be less favorable sterically. Nevertheless it is apparent from the borohydride trapping experiment at pH 1.6 that the major equilibrated iminium species must be at N-1, since only the N-1 methyl derivative is obtained under conditions where the reductive trapping is subject to thermodynamic control. The latter observation along with numerous examples of acid catalyzed condensation reactions of formaldehyde with primary and secondary aromatic amines that are postulated to involve iminium cation attack on the aromatic ring, e.g., the synthesis of Troger's base,[21] disfavors an alternative mechanism featuring formaldehyde attack at the ortho position of the exocyclic ring followed by cyclization. As noted above, it is probable that both monoprotonated and free base forms of **1a** and **2a** are precursors of **8**; the cyclization of 4-anilinopent-3-en-2-ones to give the 2,4-dimethyl-3,4-dihydroquinoline proceeds through the dicationic species.[22]

b. Benzotriazocine Formation. We previously had considered the possibility that a benzotriazocine rather than a carbinolamine at N-1 served as the precursor for imidazolidine synthesis.[1,2] Thus several aspects of the structure of **7** unequivocally synthesized from the N-1 methyl isomer, **5**, are important. First, **7** essentially is (a) a rigid molecule owing to the constraint imposed by the axially bridging *o*-phenylenediamine moiety (Figure 2); (b) exclusively in the thermodynamically favored chair conformation at room temperature; (c) in terms of the uv spectrum similar to **5**, the N-1 methyl parent amine, λ_{max} 311 vs. 312 nm (ϵ 24 800 vs. ϵ 21 800) despite the possibility for interrupted resonance; and (d) characterized by a formation constant of 1.7×10^4 M^{-1}.

The proposed structure is totally in accord with others postulated for hexahydro-1,3,5-triazines[9,23] and 1,3-hexahydropyrimidines,[24] both classes of compounds found in ground state chair conformations which are unaffected by simple N-alkyl substitution. Conformational isomerism arising in the hexahydropyrimidines from lone pair orientations on the heteroatoms, i.e., ($\alpha\alpha$) or ($\alpha\epsilon$) conformers where the lone pairs are axial-axial or axial-equatorial, respectively, are precluded in the present case by the bridging *o*-phenylenediamine. The use of **7** as an authentic indicator of the properties to be anticipated from the benzotriazocine structure therefore is justified. Several attempts to isolate the benzotriazocine formed from **1a** gave product contaminated with **2a** or a polymeric material presumably involving methylene cross linking of the N-1/N-4 quinoxaline nitrogens.[25,26]

It also is informative to compare the structure of **7** to that of **2a** or **4** (the imidazolidines), the latter deduced from the chemical shift differences $\Delta H_\alpha H_\epsilon$ for the pseudoaxial-equatorial hydrogens on the bridging methylene carbon. Chivers, Crabb, et al.[27] have established that $\Delta H_\alpha H_\epsilon$ varies from 0.1–0.2 to 0.4–0.9 ppm for imidazolidines where the C–H bond is shielded by nitrogen lone pairs oriented anti or syn, respectively. The value of $\Delta H_\alpha H_\epsilon$ for **2a** or **4** is 0.12 and 0.15 ppm, respectively. Thus **2a** apparently adopts a conformation around C-1 environmentally similar to that found for the carbon bridging N-4 and N-10 in **7**.

In a definitive paper, Sayer et al.[28] recently have proposed a general mechanism for carbinolamine formation. For amines of moderate basicity and equilibrium affinity for the carbonyl group, a stepwise pathway involving three sequential kinetically significant steps which gives rise to two negative breaks in the pH–rate profile is proposed. Owing to the limited pH range employed in these studies, only the transition at higher pH from rate-limiting solvent catalyzed proton transfer, i.e., the kinetic term, k'_4, to hydronium ion catalyzed dehydration of carbinolamine, $k^c{}_4k'_4/k'_{-4}$, would be encountered. The detection of a change in the rate-determining step at ca. pH 7 for both **1a** and **1c** as exhibited by the behavior of $k'_0/[CH_2(OH)_2]$ vs. pH (Figures 7 and 8) is in accord with the synthesis of a benzotriazocine in the initial phase through the condensation–dehydration sequence depicted in Scheme IV. Further support for the presence of benzotriazocine in the condensation of **1a** with formaldehyde to yield ultimately the imidazolidine is furnished by the successful computer simulation (Figure 9) of the optical density changes observed as a function of time in a given experiment employing the extinction coefficients obtained with the isolated benzotriazocine.[29] Thus [**1a,c**·CH_2] and [**1a,c**·CH_2OH] are designated as benzotriazocine and carbinolamine, respectively. That carbinolamine formation takes place at N-4 and not the exocyclic nitrogen is based on (a) the detection of carbinolamine formation in the conversion of **5** ⟶ **7** characterized by an equilibrium constant ($K^c{}_4$) of 23 ± 8 M^{-1}, whereas in the formaldehyde condensation with symmetrically para or meta substituted phenylethylenediamines this constant is ca. 2 M^{-1} [30] consistent with the greater sensitivity of the equilibrium for carbinolamine formation to steric rather than pK_a effects,[18] and (b) the near equality in k'_4, associated with the solvent catalyzed formaldehyde condensation, as well as in $k^c{}_4k'_4/k'_{-4}$, associated with the hydronium ion catalyzed dehydration of carbinolamine, for **1a** and **1c** (Table III) indicative of a reaction sequence at a common heteroatom unaffected by para substitution. Moreover, the last observation excludes cyclization at the N-4 iminium cation as being significantly rate limiting. Steric effects on rates and equilibria for formaldehyde condensation arising from substitution α or γ to the nitrogen are manifest (a) in the tenfold slower conversion of **5** ⟶ **7** at pH 7.0 than the corresponding reaction of **1a**, and (b) in the low value <10 M^{-1} for carbinolamine formation ($K^c{}_1$) at N-1 with **3**, the tetrahydroquinoline derivative.[17] It is apparent that similar steric effects on both the condensation and dehydration rates direct the conversion of **1a–d** to benzotriazocine formation in contrast to the generally favored formation of the five- vs. the six-membered ring system.[31]

c. Imidazolidine Formation. Two mechanistic possibilities have been considered, namely the indirect conversion of the benzotriazocines to the imidazolidines via the respective parent amines and formaldehyde, as illustrated in Scheme IV, or the direct rearrangement of the benzotriazocine to imidazolidine. The discussion will focus on the mechanism associated with the term k_0, the rate coefficient for buffer independent conversion of benzotriazocine to imidazolidine. Formaldehyde trapping of the benzotriazocine to yield imidazolidine (k^F) has not been investigated in sufficient detail to allow a mechanistic description and is simply depicted as a direct step in Scheme IV.

In order to interpret the pH–rate profiles found for the series **1a–d** after the initial phase of benzotriazocine formation in terms of the indirect pathway, it is necessary to establish the possibility that the rate-determining step(s) lies between amine and imidazolidine. This possibility is supported by the following reasoning. The computer simulation (Figure 9) of the optical density observed in the initial phase of the reaction at pH 7.4 and 6.1 for **1a** (bracketing the break in the pH–rate profile for benzotriazocine formation) sets the initial partitioning of parent amine plus formaldehyde toward benzotriazocine rather

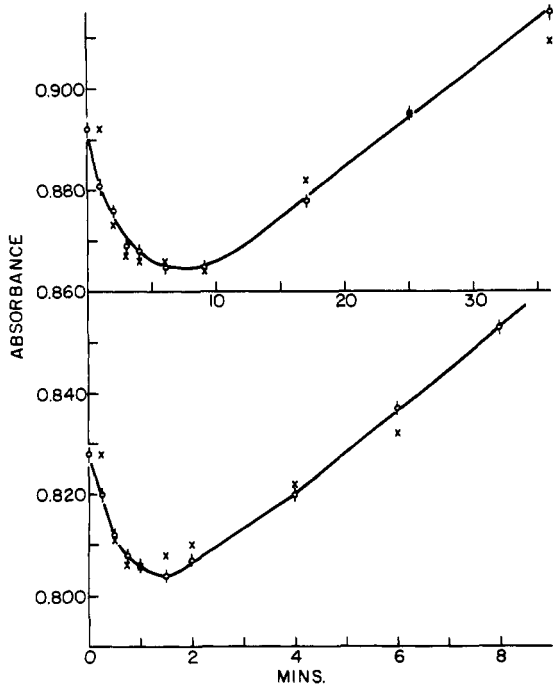

Figure 9. Computer simulation (×) of the absorbance changes (○) vs. time in the initial phase of the condensation of $CH_2(OH)_2$ with **1a**.[29] Upper curve: Phosphate, 0.05 M, pH 7.46, where $k'_{obsd} = 1.0 \times 10^3\ M^{-1}\ min^{-1}$ and $k_{obsd}K^6_{eq} = 5.28 \times 10^1\ M^{-1}\ min^{-1}$. Lower curve: Acetate, 0.2 M, pH 6.06, where $k'_{obsd} = 5.40 \times 10^3\ M^{-1}\ min^{-1}$ and $k_{obsd}K^6_{eq} = 2.37 \times 10^2\ M^{-1}\ min^{-1}$. Conditions: $[CH_2(OH)_2] = 6.15 \times 10^{-4}$ M, [**1a**] $= 3.33 \times 10^{-5}$ M, 50% v/v dioxane-water, 25 °C, $\mu = 0.2$.

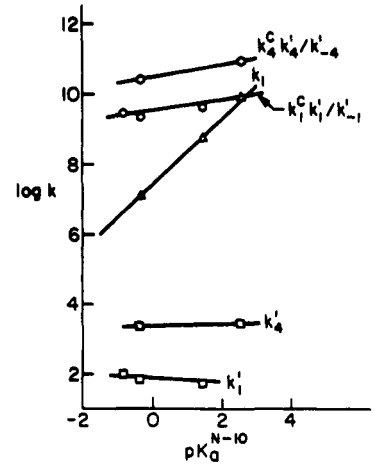

Figure 10. Structure-reactivity correlations obtained by plotting the rate coefficients (Scheme IV, Table III) against the pK_a of the exocyclic nitrogen in **1a–d**.

than imidazolidine formation as approximately 20. Moreover the reasonable agreement between K^6_{eq} for **7** and those equilibrium values obtained from plots of k_{obsd} vs. $[CH_2(OH)_2]$ for the series **1a–d** indicates that the initial formation of benzotriazocine rather than imidazolidine must be favored by at least an order of magnitude throughout the series. Thus the benzotriazocine apparently is in equilibrium with parent amine and formaldehyde throughout imidazolidine formation. Since the imidazolidines are more stable by at least an order of magnitude,[32] this aspect of the reaction system represents yet another example of the kinetic vs. thermodynamic control previously found in the tetrahydroquinoxaline model as well as tetrahydrofolate reactions on the formyl level of oxidation.[3,6] Moreover the total sequence, namely, amine plus formaldehyde → benzotriazocine → imidazolidine → benzodiazepine is an elaborate example of the interplay between thermodynamic and kinetic control.

Given the rate-determining step(s) as lying between parent amine and formaldehyde, the pH-k_0 profile for **1a** (Figure 7) may be interpreted as follows: at pH ≳7.0, rate-limiting dehydration of the N-1 carbinolamine, and at pH <7.0 rate-limiting condensation of formaldehyde with **1a** catalyzed by hydronium ion and solvent. A change in the magnitude of the catalytic coefficient associated with a given buffer is noted across the transition pH ~7.0 for the change in the nature of the rate step (Figure 6).[1] In brief this description is identical with that given above for benzotriazocine formation with the inclusion of the hydronium ion catalyzed term. Further support for this mechanism is derived from the observations that (a) the break in the profile for formation of either adduct from **1a** occurs at a similar pH; (b) the Brönsted coefficient for the general acid catalysis observed below pH 7.0 for **1a–b** and **3** is 0.2–0.3, typical of similar amine-carbonyl condensations;[33] and (c) rate coefficients for the acid-catalyzed dehydration of the carbinolamine at N-1 range from 0.4 to $8.0 \times 10^9\ M^{-1}\ min^{-1}$ in accord with values (10^9–10^{10}) found in related condensations.[34,35] The rate coefficients listed in Table III for the series **1a–d** are obtained after identifying the parametric value evaluated from eq 3 with a particular step(s) in Scheme IV. The rate equation for imidazolidine formation based on Scheme IV assuming the N-1 carbinolamine to be at steady state is given by

$$k_0 = \frac{(k_1 a_H + k'_1)k^c_1 a_H}{(k_{-1}a_H + k'_{-1} + k^c_1 a_H)K^6_{eq}} \qquad (6)$$

so that $A = k_1/K^6_{eq}$, $B = k'_1/K^6_{eq}$, and $C = k_1 k^c_1/k_{-1}K^6_{eq}$ or $k'_1 k^c_1/k'_{-1}K^6_{eq}$ where K^6_{eq} represents the equilibrium constant for benzotriazocine formation. That carbinolamine formation takes place at N-1 is based on the structure-reactivity relationships described below.

A number of interesting relationships are observed when these coefficients are plotted against the pK_a of the exocyclic amine (Figure 10), the latter measured after monoprotonation of the N-1/N-4 tetrahydroquinoxaline nitrogens.[36] First, K^6_{eq} is insensitive to the pK_a of the exocyclic nitrogen. The equilibrium constants for imidazolidine formation from neutral symmetrically para substituted diphenylethylenediamines and formaldehyde are correlated by a ρ^- value of −1.08;[29] insofar as the latter ρ value pertains to benzotriazocine formation in this series, a $\rho^- \approx -0.5$ would be anticipated.[37] Thus a total increase in K^6_{eq} of only threefold is predicted going from *p*-CN to *p*-CH_3 substitution so that the precision of the kinetic determination of K^6_{eq} (±1.0 M^{-1}) is insufficient to establish such a relationship. Second, $k^c_4 k'_4/k'_{-4}$ and $k^c_1 k'_1/k'_{-1}$, the kinetic terms for hydronium ion catalyzed dehydration of the N-4 and N-1 carbinolamines, correlate with slopes of 0.1–0.2. This term contains both the equilibrium constant for formation of the respective carbinolamines as well as the rate coefficient for their dehydration, the latter generally exhibiting $\beta_{nuc} \simeq 1.0$.[34] Consequently an increase in pK_a of less than 0.5 units at the N-1/N-4 tetrahydroquinoxaline nitrogen, accompanying the para substituent changes from CN to CH_3, would account for the observed trend solely on the basis of the latter term's high sensitivity. The macroscopic pK_a determined for monoprotonation of the tetrahydroquinoxaline moiety is 4.22, 4.33, and 4.48 (±0.05) in the series *p*-CN, *p*-COOEt, and *p*-Cl, respectively; thus the observed ΔpK_a alone is sufficient to rationalize the above result. Third, the rate coefficients, k'_1 and k'_4, for solvent catalyzed condensation of formaldehyde with **1a**, **1c**, and **1d** to form either N-1 or N-4 carbinolamine show no dependence (slopes ≃ −0.05 to 0) on the pK_a of the exocyclic nitrogen. This step exhibits $\beta_{nuc} \simeq 0.6$ for the formaldehyde–diphenylethylenediamine condensation in 50:50 v/v dioxane-H_2O;[30] therefore, the small changes in ΔpK_a

noted above would be insufficient to establish a positive correlation given the experimental precision of the data; i.e., $\Delta k'_1$ or $\Delta k'_4$ would be less than a factor of 2. In essence rate-determining steps assigned to carbinolamine dehydration or formation in either benzotriazocine or imidazolidine synthesis do not respond to alterations in the pK_a of the exocyclic nitrogen, as expected for a reaction taking place at the N-1 or N-4 nitrogen. Fourth, the hydronium catalyzed condensation of formaldehyde associated with k_1 is markedly sensitive to the pK_a of the exocyclic nitrogen with a slope of 0.9–1.0, an important observation we will consider below. It is noteworthy that the rate coefficient determined for the hydronium ion catalyzed formation of the imidazolidine adduct from **1c** falls on either the correlation for k_1 or k^c_1, in accord with the absence of a change in rate-determining step for this amine (Figure 8). Finally, if one assumes that the rates of hydrolysis of the benzotriazocine and imidazolidine adducts are similar, then the difference in $k^c_1k'_1/k'_{-1}$ and $k^c_4k'_4/k'_{-4}$ suggests the latter derivative to be more stable by an order of magnitude.

The possibility that the pH–rate profile observed for imidazolidine formation from **1a** represents an intramolecular rearrangement of the benzotriazocine to the imidazolidine as illustrated in Scheme V, with a change in the rate-determining

Scheme V

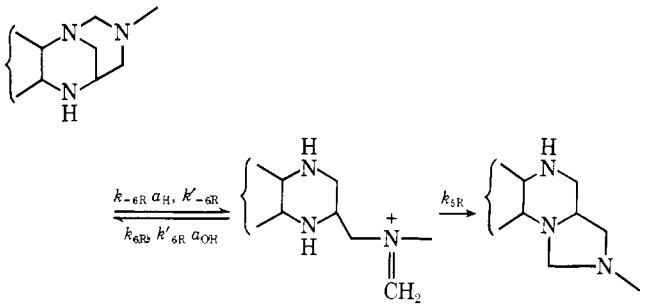

step from ring opening to cyclization, is eliminated by the following considerations.[25b] The step designated k_{-6R}, ring opening to the N-10 iminium cation, should be markedly sensitive to alterations in N-10 basicity brought about by differing para substituents. Thus this step may only be readily assigned to the hydronium ion catalyzed leg appearing at low pH, designated k_1 in Table III. However, solvent-catalyzed ring opening, k'_{-6R} evaluated as k'_1 in Table III, should likewise respond similarly to changes in para substitution which is *not* observed. An alternative but kinetically equivalent formulation of the above mechanism features solvent- and hydroxide-catalyzed ring closure steps, but then the requisite hydronium ion catalyzed ring opening step would now be associated with that leg of the pH–rate profile occurring at high pH, identified as $k'_1k^c_1/k'_{-1}$ in Table III, which also is *not* para substituent dependent. This result also is in accord with that predicted from simple symmetry considerations, namely that given the near equivalence in the basicities of N-1 and N-4, there is no basis for presuming that the partitioning of the N-10 cation between imidazolidine and benzotriazocine synthesis would change with pH. Consequently no change in the nature of the rate-determining step would be observed; i.e., there would be no break in the log k_0–pH rate profile.

Sayer et al.[28] have demonstrated that acid and solvent catalysis of carbinolamine formation may proceed through a stepwise mechanism involving formation of an unstable zwitterionic form of the carbinolamine which reverts rapidly to starting material unless it is trapped by proton transfer from acid or solvent, the latter via an intramolecular "proton switch". This stepwise mechanism for hydronium ion catalysis is formulated in Scheme VI, which gives $k_1 = (K^c_1K_a^O/K_a^{N\text{-}1})k_r$. The value of k_r computed from an estimated[38] $pK_a^O = 10.6$, $pK_a^{N\text{-}1} = 1.9$, and $K^c_1 = 10\text{–}20\ M^{-1}$ is $0.5\text{–}1 \times 10^{13}$ $M^{-1}\ s^{-1}$ and thus exceeds that found for a diffusion limited process. This difficulty may be avoided by postulating an intramolecular proton transfer from the exocyclic nitrogen thus rationalizing its effect on k_1, i.e., via the species, **10**. A value of $10^{12}\text{–}10^{13}\ s^{-1}$ may be assigned to k_r for **10** across the series

Scheme VI

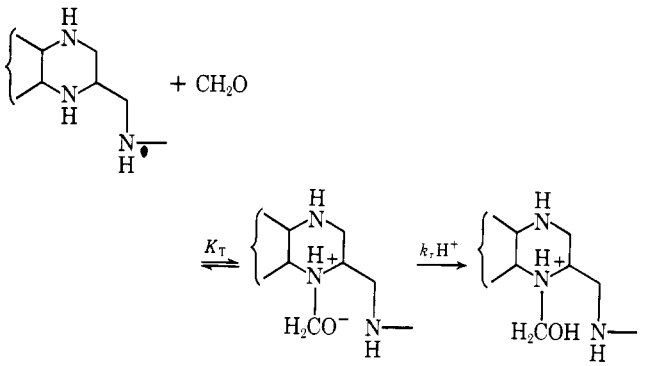

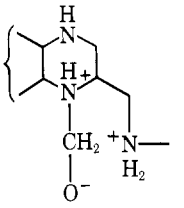

10

in accord with intramolecular proton transfer rates in the thermodynamically favorable direction.[39,40] Alternatively, a concerted process[28] may be envisioned in which carbon–nitrogen bond formation and protonation of the oxygen occur simultaneously but with proton transfer from the exocyclic nitrogen. The rate coefficient for the solvent mediated condensation calculated from Scheme VI is ca. $1\text{–}5 \times 10^7\ s^{-1}$ for **1a** consistent with a cyclic solvent mediated proton transfer process characterized by values of $10^5\text{–}10^7\ s^{-1}$ in H_2O,[28] despite the difference in solvent.

An alternative explanation for the dependence of the acid-catalyzed leg at low pH on the nature of the para substituent is a contribution to the observed rates by a hydronium-catalyzed intramolecular rearrangement of the benzotriazocines to their respective imidazolidine adducts. This pathway, however, is less favored on the following grounds. The benzotriazocines are in equilibrium with their parent amines and formaldehyde so that intermediates such as the N-4 and N-10 iminium cations likewise are at equilibrium. The N-10 iminium cation, if present, must initially cyclize to the benzotriazocine ($k_{6R} \gg k_{5R}$ in Scheme VII) so that in any rearrangement

Scheme VII

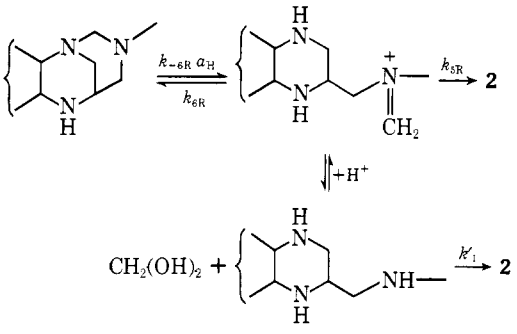

process k_{5R} would be rate limiting. Knowing that the pathway to **2** via k'_1 is favored in the pH independent region, i.e., $k'_1 \gg k_{5R}$, a route to **2** via k_{5R} cannot become important at low pH, since both the step designated k_{5R} as well as the overall equi-

librium between benzotriazocine and parent amine plus formaldehyde is pH independent. Second, trapping by $NaCNBH_3$ of the equilibrated iminium cations arising from ring opening of the imidazolidine adduct, **2a,** indicates that the cation at N-1 is present at least in 20-fold higher concentration than that at N-10, the latter being experimentally undetected despite its anticipated higher reactivity toward hydride. This observation implies that the major iminium species derived upon benzotriazocine ring opening is located at N-4, since the microscopic pK_a values for the quinoxaline nitrogens should be virtually identical.

It is significant that the cyclization step, i.e., attack by the N-10 nitrogen on the iminium cation at N-1 or N-4, does not become rate limiting in this mechanism; it is the hydration dehydration of these species that constitutes the slower steps. Moreover direct rearrangement of the six- to five-membered ring adducts is not dominant despite a conformation (Figure 2) suitably poised for such a process. Thus it appears quite plausible that initial ring opening of **7** or **2** is mainly in the direction of the more stable cation. Presuming a late transition

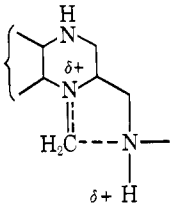

state for this process, the degree of protonation of the less basic exocyclic nitrogen would then be directly offset by its being a more favorable leaving group ($\beta_{lg} = -1.0$), so that cation stability dictates the direction of the ring opening. The para substituted triaryl- or diarylcarbinol-carbonium ion equilibrium is characterized by ρ values of -3.5 and -6.7, respectively;[37] for equilibrium protonation of para and meta substituted anilines (H_2O) $\rho^- = -2.81$[41] so that the above ρ^- is at least greater than 3.0. Although a reliable value for an *o*-NH_2 group is not available, it is reasonable that electron donation by this substituent contributes throughout the **2a–d** series, so that ring opening favors the N-1/N-4 iminium cation species. However, for **2a** the effect of the para substituent on lowering the N-10 electron density alone is sufficient to direct the course of ring opening. Thus in contrast to reactions at the formyl level of oxidation, the direction of ring opening favors expulsion of the less basic nitrogen.[3,6]

Conclusion

The above results permit the following comments on the properties of the 5,10-methylenetetrahydrofolate cofactor as well as its mechanism of formation: (1) the similarity between k_1, k'_1, and $k'_1k^c_1/k'_{-1}$ for **1a** and the corresponding terms for the condensation of formaldehyde with tetrahydrofolate in water (2.8×10^7, 5.4×10^3, and 5.2×10^{10} M^{-2} min^{-1}, respectively)[42,43a] suggests that proton transfer from N-10 rather than hydronium ion may catalyze the condensation reaction as well as loss of formaldehyde so that the cofactor itself may catalyze one carbon unit transfer in some enzymatic cases;[44] (2) the results of the borohydride trapping, the observation of benzodiazapene formation, as well as the absence of intramolecular rearrangements for **2a** are consistent with preferential ring opening to the N-5 iminium cation for the cofactor probably for kinetic and certainly for thermodynamic control (borohydride reduction of the cofactor yields 5-methyltetrahydrofolate exclusively[45]); and (3) the lower nucleophilicity of N-8 owing to conjugation with the pyrimidine ring avoids benzotriazocine formation as well as protonation.[1] These conclusions are only accessible via studies of dissymmetric systems.

Experimental Section

Infrared spectra were taken on a Perkin-Elmer Model 257 and were calibrated with polystyrene film. Nuclear magnetic resonance spectra were taken on Varian Associates HA-100 and A-60 instruments and chemical shifts are reported in δ units relative to tetramethylsilane. The 250-MHz NMR spectra of **7**-d_2 were provided by the Mellon Institute of Science, Pittsburgh, Pa. Ultraviolet spectra were taken on a Cary 14 instrument. Elemental analyses were performed by Midwest Microlab, Ltd., Indianapolis, Ind. Solvents were reagent grade and used as received. Melting points were taken with a Fisher-Johns melting point apparatus and are uncorrected. Dioxane used in the kinetic runs was purified by the method of Fieser[46] and freshly distilled from sodium for each day's runs. Doubly distilled, deionized water was employed. Formaldehyde solutions were prepared daily from a standard solution of formaldehyde, the titer of which was checked routinely.[47]

Materials. The synthesis of the tetrahydroquinoxaline compounds **1a–c** and **2a–c** as well as the tetrahydroquinoline derivatives **3** and **4** has been described previously.[1,2] Preparation of *p*-[[(1,2,3,4-tetrahydro-2-quinoxalinyl)methyl]amino]benzonitrile (**1d**) was identical with the procedure employed earlier: mp 152–153 °C; λ_{max} (H_2O) (pH 7.8) 290 nm (ϵ 28 400); NMR (DMSO-d_6, 60 MHz) δ 6.92 (AB quartet, J_{ab} = 9 Hz, 4 H), 6.33 (s, 4 H), 3.0–3.6 (multiplet, 5 H).

Anal. Calcd for $C_{16}H_{16}N_2$: C, 72.69; H, 6.11; N, 21.20. Found: C, 73.14; H, 6.12; N, 20.83.

The imidazolidine (**2d**) was prepared according to published procedures:[1,2] mp 129–131 °C; λ_{max} (H_2O) (pH 7.8) 290 nm (ϵ 32 000); NMR (dioxane, 60 MHz) δ 7.05 (AB quartet, J_{ab} = 9 Hz, 4 H), 6.55 (s, 4 H), 4.72 (AB quartet, J_{ab} = 4 Hz, 2 H), 2.7–3.2 (multiplet, 5 H). The purity of the tetrahydroquinoxaline derivatives was analyzed on silica gel TLC (Brinkmann PF-254) by migration with ethyl acetate:cyclohexane (4:1, v/v) and visualization with uv light or by spraying with 5% $FeCl_3$ in 0.1 N HCl. The ferric chloride spray produced characteristic colors which were stable for about 0.5 h.

Ethyl *p*-[[(1,2,3,4-Tetrahydro-1-methyl-2-quinoxalinyl)methyl]amino]benzoate (5). Ethyl *p*-(3,4,4a,5-tetrahydroimidazo[1,5-*a*]quinoxalin-2(1*H*)-yl)benzoate (**2a**) (500 mg, 1.5 mmol) was dissolved in dioxane (50 ml) with magnetic stirring and water (5 ml) was added. The acidity of the solution was monitored with a pH meter (Radiometer). Sodium cyanoborohydride (Alfa Inorganics) (10 mg, 1.61 mmol) was added followed by 0.1 N HCl as needed to maintain a constant reading on the meter. After the meter reading remained stable for several minutes the solution was made basic with 0.1 N KOH and evaporated in vacuo to dryness. The residue was dissolved in benzene (30 ml), washed with water (2 × 15 ml), dried (anhydrous K_2CO_3), and evaporated in vacuo to give a yellow oil. The sample was placed on a column of silica gel (2.5 × 25 cm, 100 g mesh 100–200) and eluted with ethyl acetate:cyclohexane (4:1, v/v). Fractions were monitored by TLC (R_f 0.66, maroon to ferric chloride). The pooled fractions containing product were evaporated in vacuo to a colorless gum which solidified upon cooling overnight (116 mg, 23%). Recrystallization from 2-propanol gave colorless crystals: mp 106–107 °C; ir (Nujol) 3350, 1680, 1600 cm^{-1}; uv λ_{max} 50% v/v dioxane–water (pH 7.0) 312 nm (ϵ 24 800); NMR ($CDCl_3$, 100 MHz) δ 7.81 and 6.56 (qAB, J = 9 Hz), 6.80 to 6.35 (m) (8 H); 4.54 (s, broad, 2 H), 4.27 (q, 2 H, J = 7 Hz), 3.52 to 3.15 (m, 5 H), 2.93 (s, 3 H), 1.36 (t, 3 H, J = 7 Hz); *m/e* 325 (M^+).

Anal. Calcd for $C_{19}H_{23}N_3O_2$: C, 70.15; H, 7.07; N, 12.92. Found: C, 70.12; H, 7.14; N, 12.85.

Ethyl *p*-[Methyl[(1,2,3,4-tetrahydro-2-quinoxalinyl)methyl]amino]benzoate (6). Boron trifluoride etherate (Eastman) was redistilled under vacuum from calcium hydride (Ventron). The purified boron trifluoride etherate (0.75 ml, 6.0 mmol) was added slowly through a septum to a magnetically stirring mixture of excess sodium borohydride (Alfa Inorganics) (325 mg, 8.7 mmol) and tetrahydrofuran (150 ml) maintained at 0 °C. The mixture was allowed to warm to room temperature. The N-10 formyl derivative of **1a**[3] (500 mg, 1.47 mmol) dissolved in tetrahydrofuran (20 ml) was added slowly to the mixture and stirring continued for 20 min. HCl (2 ml 6 N) was added dropwise and after another 20 min the solution was made basic with $NaHCO_3$, extracted with ether (2 × 50 ml), washed (50 ml H_2O), dried ($MgSO_4$), and evaporated in vacuo to give a colorless oil. The sample was dissolved in a minimum amount of ethyl acetate, placed on a column of silica gel (2.5 × 35 cm, 100 g), and eluted with ethyl acetate:cyclohexane (4:1, v/v). Fractions were monitored by TLC (R_f

0.62, dark purple to ferric chloride). The pooled fractions containing product were evaporated in vacuo to a colorless gum which solidified upon addition of a few drops of 2-propanol (145 mg, 30%). Recrystallization from 2-propanol gave colorless crystals: mp 92–94 °C; ir (Nujol) 3320, 3250 (b), 1685, and 1600 cm^{-1}; uv λ_{max} (EtOH) 314 nm (ϵ 31 400) and 222 nm (ϵ 36 400); NMR ($CDCl_3$, 100 MHz) δ 7.87 and 6.68 (qAB, J = 9 Hz), 6.60 to 6.35 (m) (8 H); 4.31 (q, 2 H, J = 7 Hz), 3.85 to 3.10 (m, 7 H), 3.05 (s, 3 H), 1.34 (t, 3 H, J = 7 Hz); *m/e* 325 (M^+).

Anal. Calcd for $C_{19}H_{23}N_3O_2$: C, 70.15; H, 7.07; N, 12.92. Found: C, 69.94; H, 7.27; N, 12.75.

Ethyl *p*-(5,6-Dihydro-6-methyl-2*H*-1,5-methano-1,3,6-benzotriazocin-3(4*H*)-yl)benzoate (7). The N-1 formyl derivative of **1a** (200 mg, 0.59 mmol) was reduced with diborane in situ as described above for the N-10 isomer. The reduction product was dissolved in tetrahydrofuran (10 ml) and water added (2 ml) followed by several drops of formaldehyde (Fisher, 37%). The solution was evaporated in vacuo, redissolved in ethyl acetate, placed on a column of silica gel, and eluted with TLC monitoring as described above (R_f 0.43, dark red to ferric chloride). The pooled fractions containing product were evaporated in vacuo to a colorless gum which solidified upon addition of a few drops of 2-propanol (92 mg, 46%). Recrystallization from 2-propanol gave colorless crystals: mp 114–115 °C; ir (Nujol) 1690 and 1600 cm^{-1}; uv λ_{max} 50% v/v dioxane–water (pH 7.0) 311 (ϵ 21 800) and 258 nm (ϵ 11 300); NMR ($CDCl_3$, 100 MHz) δ 7.73 and 6.49 (qAB, J = 9 Hz), 7.26 to 6.35 (m) (8 H); 4.84 and 4.32 (qAB, J = 12 Hz), 4.25 (q, J = 7 Hz) (4 H); 4.01 and 3.47 (qAB, J = 13 Hz), 3.44 to 3.04 (m) (5 H); 2.98 (s, 3 H), and 1.32 (t, 3 H, J = 7 Hz); *m/e* 337 (M^+).

Anal. Calcd for $C_{20}H_{23}N_3O_2$: C, 71.21; H, 6.82; N, 12.46. Found: C, 71.27; H, 6.96; N, 12.47.

The above compound is identical with a sample prepared by addition of formaldehyde to a pure sample of **5** dissolved in tetrahydrofuran. Dideuterioformaldehyde prepared from hydrolysis of paraformaldehyde-d_2 (Merck) was added to a solution of **5** to yield the dideuterio adduct. After purification by silica gel column chromatography and recrystallization from 2-propanol, this compound was identical in mp and TLC with **7**. The mass spectrum gave the molecular ion peak at *m/e* 339. An NMR spectrum of **7**-d_2 in the region of 4.0 to 3.1 ppm obtained at 250 MHz is shown in Figure 1.

2-Carbethoxy-5,6,7,8-tetrahydro-14*H*-quinoxo[2,1-*c*][1,4]benzodiazepine (8). Compound **8** was prepared in the same manner as **9** using a solution of **2a** (323 mg, 1.0 mmol) in dioxane (200 ml) except that 5.1 N H_2SO_4 was employed and the reaction allowed to proceed for 10 h at 25 °C. Recrystallization from petroleum ether–benzene yielded white crystals (209 mg, 65%): mp 208–210 °C; NMR ($CDCl_3$, 60 MHz) δ 8.05 (s, 1 H), 7.75 (d, 1 H, J = 9 Hz), 6.85 to 6.40 (m, 5 H), 4.45 (s, 2 H), 4.40 (q, 2 H, J = 7 Hz), 4.00 to 3.15 (m, 7 H), and 1.38 (t, 3 H, J = 7 Hz); *m/e* 323 (M^+).

Anal. Calcd for $C_{19}H_{21}N_3O_2$: C, 70.56; H, 6.54; N, 12.98. Found: C, 69.90; H, 6.75; N, 12.67.

2-Carbethoxy-5,6,7,8-tetrahydro-14*H*-quino[2,1-*c*][1,4]benzodiazepine (9). A solution of **4** (322 mg, 1.0 mmol) in dioxane (200 ml) was added to a four-necked 500-ml round-bottom flask fitted with an addition funnel, rubber septum, and nitrogen gas inlet and outlet tubes. The addition funnel was charged with 200 ml of aqueous acid (1.39 N H_2SO_4) and the apparatus flushed with nitrogen. The reaction was initiated by rapid addition of the acid and stirred for 3 h at 55 °C. After addition of several drops of mercaptoethanol, the reaction solution was slowly added to a rapidly stirring 10% aqueous solution of sodium bicarbonate (400 ml), extracted with ether (3 × 100 ml), dried ($MgSO_4$), and evaporated in vacuo to give a yellow residue. The residue was dissolved in a minimum of benzene, added to a 1.25 × 15 cm chromatographic column of activated alumina (mesh 100, Fisher), and eluted with 180 ml of benzene. The eluent was evaporated in vacuo to a white solid (225 mg, 70%). Recrystallization from benzene–petroleum ether gave white crystals: mp 118–119 °C; ir (Nujol) 3400 cm^{-1}; uv λ_{max} (EtOH) 302 (ϵ 22 000), 259 (ϵ 16 400), and 225 nm (ϵ 12 800); NMR ($CDCl_3$, 60 MHz) δ 7.95 (s, 1 H), 7.60 (d, 1 H, J = 8 Hz), 7.10 to 6.30 (m, 5 H), 4.58 (s, 2 H), 4.35 (q, 2 H, J = 7 Hz), 4.00 to 2.50 (m, 6 H), 2.10 to 1.70 (m, 2 H), and 1.38 (t, 3 H, J = 7 Hz); *m/e* 322 (M^+).

Anal. Calcd for $C_{20}H_{22}N_2O_2$: C, 74.66; H, 6.83; N, 8.70. Found: C, 74.70; H, 7.00; N, 8.67.

Trapping Experiments. Compounds **2a**, **5**, and **6** and mixtures of **5** and **6** (80:20, 90:10, and 95:5% **5**:**6**) were dissolved in tetrahydrofuran to give 1.85×10^{-2} M stock solutions. Sodium cyanoborohydride was dissolved in distilled water to give 0.18 and 0.37 M stock solutions that were freshly prepared before each use. Buffers were made with 50% v/v dioxane (0.2 M, μ = 0.2, KCl) at pH 1.60 (trichloroacetate), 4.20 (formate), and 7.27 (phosphate, 0.05 M).

The trapping experiment was initiated by injecting 10 μl of stock solution followed immediately by 10 μl of reducing agent into 0.10 ml of buffer at room temperature. Reversing the order of addition, increasing the concentration of reducing agent, or aging the solution for several minutes prior to addition of reducing agent had no effect on the product distribution. The solution was then evaporated in vacuo to dryness, extracted with tetrahydrofuran, concentrated to a small volume, spotted at one corner of a 20 × 20 cm TLC plate (Brinkmann PF-254 silica gel), migrated with ethyl acetate:cyclohexane (4:1, v/v), and allowed to dry completely. The plate was then rotated 90°, sprayed lightly with formaldehyde (0.13 M) while masking all but the lower edge, allowed to dry, migrated with the same solvent, and sprayed with ferric chloride solution.

After demonstration that the control samples are unchanged by the above treatment at each pH, they were spotted alongside the reduction product prior to application of formaldehyde. Conversion of **5** to **7** is quantitative and permits reliable detection of **6** at 5% in the presence of **5**. Under identical conditions the reduction reaction was complete at pH 1.60 but somewhat less than complete at pH 4.20 and 7.27 as estimated by the appearance of residual **2a** (R_f 0.63, bright blue to ferric chloride).

Kinetics. The instruments employed have been previously described.[1,2] The pseudo-first-order rates (k_{obsd}) for reduction of **2a** with sodium cyanoborohydride were determined spectrophotometrically from the time-dependent decrease in absorbance at 310 nm. Reactions were initiated by injecting 20 μl of stock solution of **2a** in dioxane into 2 ml of 0.10 M acetate buffer (50% v/v dioxane, μ = 0.1, 25 °C, pH 4.80) containing sodium cyanoborohydride. The final concentration of substrate was 2×10^{-5} M. The k_{obsd} remained first order in sodium cyanoborohydride concentration as the latter was varied from 1.0×10^{-4} to 4.9×10^{-3} M. It was not possible to examine the reaction at greater concentration due to the high value for k_{obsd} and the dark color of the solution.

The hydrolysis of **7** was carried out in buffered solutions (50% v/v dioxane-phosphate, pH 7.0, μ = 0.2, 25 °C) containing 0.02, 0.05, and 0.10 M mercaptoethanol with a substrate concentration of 5×10^{-5} M and was independent of mercaptoethanol concentration. The reaction was monitored by the time-dependent increase in absorbance at 312 nm. Rates were extrapolated to zero buffer concentration. Similarly, the formation of **7** from **5** and formaldehyde was monitored by the time-dependent decrease in absorbance at 312 nm (50% v/v dioxane–phosphate, pH 7.0, μ = 0.2, 25 °C, 5×10^{-5} M substrate). Formaldehyde concentration was varied from 1.3×10^{-3} to 0.30 M and the rates were extrapolated to zero buffer concentration.

The measurement of the pseudo-first-order rate constants for formation of **2d** and the benzotriazocines derived from **1a** and **1c** were monitored at 290, 310, and 255 or 310 nm, respectively. An experimental protocol identical with that described in detail in ref 1 was followed. All kinetic runs were in 50% v/v dioxane–water, μ = 0.2 with KCl, 25 °C. The validity of employing glass electrode measurements as an index of hydrogen ion activity in this solvent has been demonstrated by Purlee and Grunwald.[48] Measurement of benzodiazepine formation (**8**) was monitored at 300 nm in aqueous solution; the hydronium ion activity was determined relative to H_0.[49] All values for k_{obsd} were computed from log plots ($OD_\infty - OD_t$) vs. time with a precision of ±5%.

Crossover Experiments. The experimental protocol followed for a typical crossover experiment was as follows: a 50-ml dioxane solution containing 0.1 mmol of **2a** or **4** was preequilibrated in the apparatus described for **9**. Standardized aqueous formaldehyde (h_2 or d_2) at the desired concentration (after correction for dilution) was then injected, followed by standardized aqueous acid to initiate the reaction (total volume 100 ml). The resulting solution was incubated at 55 °C for 3–24 h and worked up as described above. The pH of the solution was determined prior to workup.

A mass spectral method was used to determine the degree of formaldehyde (d_2 or h_2) incorporated into **8** or **9**. For **9** the ratio of parent peak intensities 324/322 was equated with the concentration ratio of the dideuterio to diprotio material; in the case of **8** the ratio 325/323 was employed. This ratio was corrected for *m/e* contributions arising from the P + 2 peak of the h_2 species and the P − 2 peak arising

from the d_2 species calculated from the mass spectra of the pure h_2 or d_2 isomers. In addition control experiments were carried out with the benzodiazepine products in order to correct for their possible exchange with medium formaldehyde under the conditions of the experiment. The latter proved to be less than 5% for both **8** and **9**. The equations employed have been published elsewhere.[19]

Note Added in Proof: direct rearrangement of benzotriazocine to imidazolidine may occur with increased N-10 basicity (greater than **1c**) and should be manifest by a deviation from the correlations in Figure 10.

Acknowledgment. This work was supported by a grant to S.J.B. from the National Science Foundation. We are indebted to Dr. M. M. deMaine for carrying out the CRAMS simulation.

References and Notes

(1) S. J. Benkovic, P. A. Benkovic, and D. R. Comfort, *J. Am. Chem. Soc.*, **91,** 5270 (1969).
(2) S. J. Benkovic, P. A. Benkovic, and R. Chrzanowski, *J. Am. Chem. Soc.*, **92,** 523 (1970).
(3) S. J. Benkovic, W. P. Bullard, and P. A. Benkovic, *J. Am. Chem. Soc.*, **94,** 7542 (1972).
(4) H. C. Brown and P. Heim, *J. Org. Chem.*, **33,** 912 (1973).
(5) G. Zweifel and H. C. Brown, *Org. React.*, **13,** 1 (1963).
(6) S. J. Benkovic, T. H. Barrows, and P. R. Farina, *J. Am. Chem. Soc.*, **95,** 8414 (1973).
(7) T. S. Moore and I. Doubleday, *J. Chem. Soc.*, **119,** 1170 (1921).
(8) F. G. Riddell, *J. Chem. Soc. B*, 560 (1967).
(9) J. M. Lehn, F. G. Riddell, B. J. Price, and I. O. Sutherland, *J. Chem. Soc. B*, 387 (1967).
(10) L. M. Jackman and S. Sternhell, "Applications of Nuclear Magnetic Resonance Spectroscopy in Organic Chemistry", 2nd ed, Pergamon Press, London, 1969.
(11) The observed constants obtained from a scale expanded portion of the spectrum (not shown) in the region of 3.1 to 3.5 ppm are all within 1.8 ± 0.3 Hz. The coupling constants obtained from the splitting at δ 4.0 are apparently 2.0 Hz but are reported with less confidence since a scale expansion of this region was not obtained.
(12) R. M. Silverstein and G. C. Bassler, "Spectrometric Identification of Organic Compounds", 2nd ed, Wiley, New York, N.Y., 1967, p 92.
(13) R. F. Borch, M. D. Berstein, and H. D. Durst, *J. Am. Chem. Soc.*, **93,** 2897 (1971).
(14) The traces of OD vs. time for formation of **8** show either an initial rapid decrease in OD at 300 nm commencing the reaction with **1a** and $CH_2(OH)_2$ or an initial rapid increase beginning with **2a** that is complete before any significant production of **8**. A common intermediate OD value is attained dependent on pH. Such behavior is consistent with the establishment of a preequilibrium between **2a** and **1a** as required by Scheme I.
(15) Formaldehyde is nearly completely hydrated in aqueous solution, but its rate of dehydration to free formaldehyde would not be rate limiting under the conditions of this study: P. LeHénaff, *C. R. Hebd. Seances Acad. Sci.*, 1752 (1963).
(16) E. A. Halevi, *Prog. Phys. Org. Chem.*, **1,** 109 (1963).
(17) P. A. Benkovic, unpublished results.
(18) R. G. Kallen and W. P. Jencks, *J. Biol. Chem.*, **241,** 5864 (1966); J. DeLuis, Ph.D. Thesis, The Pennsylvania State University, 1964.
(19) R. Chrzanowski, Ph.D. Thesis, The Pennsylvania State University, 1971.
(20) R. Taylor, "Comprehensive Chemical Kinetics", Vol 13, C. H. Bamford and C. F. H. Tipper, Ed., Elsevier, Amsterdam, 1972, Chapter 1.
(21) W. V. Farrar, *Chem Ind. (London)*, 1644 (1967); W. V. Farrar, *J. Appl. Chem.*, **14,** 389 (1964).
(22) T. G. Bonner and M. Barnard, *J. Chem. Soc.*, 4181 (1958).
(23) F. Bohlmann, D. Schuman, and C. Arnt, *Tetrahedron Lett.*, 2705 (1965).
(24) S. F. Nelsen and J. M. Buschek, *J. Am. Chem. Soc.*, **96,** 7930 (1974); E. L. Eliel, L. D. Kopp, J. E. Dennis, and S. A. Evans, Jr., *Tetrahedron Lett.*, 3409 (1971); R. A. Y. Jones, A. R. Katritzky, and M. Shorey, *J. Chem. Soc. B*, 1 (1970).
(25) (a) The claim that the benzotriazocine derived from **1a** has been isolated is dubious given the need to rationalize the poor quality NMR spectrum in terms of a boat–chair equilibrium as well as the absence of further purification of the crude material. (b) G. P. Tuszynski and R. G. Kallen, personal communication.
(26) T. H. Barrows, Ph.D. Thesis, The Pennsylvania State University, 1974.
(27) P. V. Chivers, T. A. Crabb, and R. O. Williams, *Tetrahedron*, **25,** 2921 (1969) and references therein.
(28) J. M. Sayer, B. Pinsky, A. Schronbrum, and W. Washtien, *J. Am. Chem. Soc.*, **96,** 7998 (1974).
(29) (a) The computer simulation was based on the following equation

$$\text{benzotriazocine} \underset{k'_{obsd}}{\overset{k'_{-obsd}}{\rightleftharpoons}} \mathbf{1a} + CH_2(OH)_2 \xrightarrow{k_{obsd}K^6_{eq}} \text{imidazolidine}$$

where k'_{obsd} and k_{obsd} are the experimentally determined pseudo-first-order rate coefficients for the initial and latter phases of the condensation reaction. The value of k'_{-obsd} was computed from $K^6_{eq} = k'_{obsd}/k'_{-obsd}$ where $K^6_{eq} = 5.5 \pm 2.0 \times 10^3\ M^{-1}$. The extinction coefficients employed were 2.81×10^4 (**1a**), 2.47×10^4 (benzotriazocine), and 3.29×10^4 (imidazolidine). The value for the benzotriazocine was calculated from the ratio of the ϵ for **7**/**5** times the ϵ for **1a**. The CRAMS program described previously was employed: (b) R. Fishbein, P. A. Benkovic, K. J. Schray, I. J. Siewers, J. J. Steffens, and S. J. Benkovic, *J. Biol. Chem.*, **249,** 6047 (1974).
(30) G. P. Tuszynski and R. G. Kallen, *J. Am. Chem. Soc.*, **97,** 2860 (1975).
(31) E. L. Eliel, "Stereochemistry of Carbon Compounds", McGraw-Hill, New York, N.Y., 1962.
(32) The equilibrium constant for imidazolidine formation from formaldehyde and diphenylethylenediamine (50% v/v dioxane–H_2O, μ = 0.1, 25 °C) is $1.3 \times 10^5\ M^{-1}$, ref 30.
(33) R. G. Kallen, *J. Am. Chem. Soc.*, **93,** 6227, 6236 (1971), and references therein; M. I. Page and W. P. Jencks, *ibid.*, **84,** 832 (1962).
(34) W. P. Jencks, "Catalysis in Chemistry and Enzymology", McGraw-Hill, New York, N.Y., 1969.
(35) A value of $6.6 \times 10^9\ M^{-1}\ min^{-1}$ has been found for the hydronium ion catalyzed dehydration of the carbinolamine derived from formaldehyde and diphenylethylenediamine.[30]
(36) The values employed for **1a**, **1b**, and **1d** were obtained by spectrophotometric titration. The value used for **1c** was estimated from the empirical relationship $pK_a^{N\text{-}10} = pK_{a(H_2O)} - 2.5$ where $pK_{a(H_2O)}$ is that for the corresponding para-substituted aniline.
(37) H. H. Jaffee, *Chem. Rev.*, **53,** 191 (1953).
(38) The pK_a of the nitrogen and oxygen atoms for the carbinolamine formed with the tetrahydroquinoxaline derivatives was estimated by the procedures of Sayer and Jencks.[38a] For the oxygen (pK_a^O) starting with an estimated pK_a^O of 10.0 for $CH_3N^+H_2CH_2OH$,[38b] replacement of a CH_3 by *o*-phenylenediamine should give a ΔpK of −1.1[38c] after correction for fall off factors of 2.5 and 2.0 for transmission through carbon and nitrogen, respectively. Allowance for the effect of the mixed solvent on oxyanion ionization, based on ΔpK_a observed for carboxylic and phosphate buffers, provides +1.7 pK_a units. Thus pK_a^O is estimated as 10.6. The $pK_a^{N\text{-}1} = 1.9$ is calculated from the macroscopic pK_a for N-1/N-4 (3.78) in the mixed solvent adjusted by $\Delta pK_a = -1.9$ for hydroxymethyl substitution.[30] K_1^c is defined as the equilibrium constant for formation of neutral carbinolamine from the free base form of the amine plus formaldehyde and lies in the range 10–20 M^{-1}. (a) J. M. Sayer and W. P. Jencks, *J. Am. Chem. Soc.*, **95,** 5637 (1973); (b) J. Hine, J. C. Craig, J. G. Underwood, II, and F. A. Via, *ibid.*, **92,** 5194 (1970); (c) A. Albert and E. P. Serjeant, "The Determination of Ionization Constants", Chapman and Hall, London, 1971.
(39) M. Eigen, *Angew. Chem., Int. Ed. Engl.*, **3,** 1 (1964).
(40) The expression for $k_r = k_1K_a^{N\text{-}1}K_a^{N\text{-}10}/K^c{}_1K_a^O$ where $a_H < K_a^{N\text{-}10}$.
(41) A. I. Biggs and R. A. Robinson, *J. Chem. Soc.*, 388 (1961).
(42) R. G. Kallen and W. P. Jencks, *J. Biol. Chem.*, **241,** 5851 (1966).
(43) (a) Differences in these parameters may be mainly ascribed to pK_a differences between the model and tetrahydrofolate at N-1(5) and N-10. In tetrahydrofolate, $pK_a^{N\text{-}5} = 4.8$ and $pK_a^{N\text{-}10} = -1.3$. (b) R. G Kallen and W. P. Jencks, *J. Biol. Chem.*, **241,** 5845 (1966).
(44) S. J. Benkovic and W. P. Bullard, "Progress in Bioorganic Chemistry", Vol. 2, E. T. Kaiser and F. J. Kezdy, Ed., Wiley-Interscience, New York, N.Y., 1973.
(45) V. S. Gupta and F. M. Huennekens, *Arch. Biochem. Biophys.*, **120,** 712 (1967).
(46) L. F. Fieser, "Experiments in Organic Chemistry", 3rd ed, D. C. Heath, Boston, Mass., 1955, p 284.
(47) J. F. Walker, *ACS Monogr.*, 159 (1964).
(48) E. L. Purlee and E. Grunwald, *J. Am. Chem. Soc.*, **79,** 1366 (1957).
(49) N. A. Paul and F. A. Long, *Chem. Rev.*, **1,** 57 (1957).